



## ORIGINAL ARTICLE

# TAS2940, a novel brain-penetrable pan-ERBB inhibitor, for tumors with *HER2* and *EGFR* aberrations

Kei Oguchi<sup>1,2</sup>  | Hikari Araki<sup>1</sup> | Shingo Tsuji<sup>1</sup> | Masayuki Nakamura<sup>1</sup> | Akihiro Miura<sup>1</sup> | Kaoru Funabashi<sup>1</sup> | Akiko Osada<sup>1</sup> | Sakiho Tanaka<sup>1</sup> | Takamasa Suzuki<sup>1</sup> | Susumu S. Kobayashi<sup>2,3,4</sup>  | Shinji Mizuarai<sup>1</sup>

<sup>1</sup>Discovery and Preclinical Research Division, Taiho Pharmaceutical Co., Ltd, Tsukuba, Japan

<sup>2</sup>Department of Integrated Biosciences, Graduate School of Frontier Sciences, The University of Tokyo, Kashiwa, Japan

<sup>3</sup>Division of Translational Genomics, Exploratory Oncology Research and Clinical Trial Center, National Cancer Center, Kashiwa, Japan

<sup>4</sup>Division of Hematology/Oncology, Department of Medicine, Beth Israel Deaconess Medical Center, Harvard Medical School, Boston, Massachusetts, USA

## Correspondence

Shinji Mizuarai, Discovery and Preclinical Research Division, Taiho Pharmaceutical Co., Ltd., 3 Okubo, Tsukuba, Ibaraki 300-2611, Japan.

Email: [s-mizuarai@taiho.co.jp](mailto:s-mizuarai@taiho.co.jp)

Susumu S. Kobayashi, Division of Translational Genomics, Exploratory Oncology Research and Clinical Trial Center, National Cancer Center, 6-5-1 Kashiwanoha, Kashiwa, Chiba 277-8577, Japan.

Email: [sukobaya@east.ncc.go.jp](mailto:sukobaya@east.ncc.go.jp)

## Funding information

Taiho Pharmaceutical

## Abstract

Genetic alterations in human epidermal growth factor receptor type 2 (*HER2*)/epidermal growth factor receptor (*EGFR*) are commonly associated with breast and lung cancers and glioblastomas. Cancers with avian erythroblastosis oncogene B (*ERBB*) deregulation are highly metastatic and can cause primary brain tumors. Currently, no pan-*ERBB* inhibitor with remarkable brain penetration is available. Here, TAS2940, a novel irreversible pan-*ERBB* inhibitor with improved brain penetrability, was evaluated for its efficacy against several *ERBB* aberrant cancer models. The selectivity of TAS2940 was evaluated by enzymatic kinase assays. The inhibitory effects of TAS2940 against *ERBB* genetic alterations were examined using MCF10A cells expressing various *HER2* or *EGFR* mutations and other generic cell lines harboring deregulated *ERBB* expression. In vivo efficacy of TAS2940 was examined following oral treatment in subcutaneous or intracranial xenograft cancer models. TAS2940 was highly potent against cells harboring *HER2/EGFR* alterations. TAS2940 could selectively inhibit phosphorylation of targets and the growth of cancer cells with *ERBB* aberrations in vitro. TAS2940 also inhibited tumor growth in xenograft mouse models with *ERBB* aberrations: *HER2* amplification, *HER2/EGFR* exon 20 insertions, and *EGFR* vIII mutation. TAS2940 was effective in the intracranial xenograft models of *HER2/EGFR* cancers and improved the survival of these mice. TAS2940 has promising therapeutic effects in preclinical study against cancers harboring *HER2/EGFR* mutations, especially metastatic and primary brain tumors. Our results highlight potential novel strategies against lung cancers with brain metastases harboring *HER2/EGFR* exon 20 insertions and glioblastomas with *EGFR* aberrations.

## KEYWORDS

brain penetration, EGFR, exon 20 insertion, HER2, TAS2940

**Abbreviations:** AUC<sub>last</sub>, area under the plasma concentration-time curve from time 0 to the last quantifiable time point; C<sub>max</sub>, maximum plasma concentration; EGFR, epidermal growth factor receptor; ERBB, avian erythroblastosis oncogene B; HER2, human epidermal growth factor receptor type 2; HPMC, hydroxypropyl methylcellulose; LC-MS, liquid chromatography-mass spectrometry; LC-MS/MS, liquid chromatography-tandem mass spectrometry; MST, median survival time; NSCLC, non-small-cell lung cancer; PARP, poly(ADP-ribose) polymerase; PD, pharmacodynamic; TKI, tyrosine kinase inhibitor; TV, tumor volume.

This is an open access article under the terms of the [Creative Commons Attribution-NonCommercial](https://creativecommons.org/licenses/by-nc/4.0/) License, which permits use, distribution and reproduction in any medium, provided the original work is properly cited and is not used for commercial purposes.

© 2022 Taiho Pharmaceutical Co., Ltd and The Authors. *Cancer Science* published by John Wiley & Sons Australia, Ltd on behalf of Japanese Cancer Association.

## 1 | INTRODUCTION

Epidermal growth factor receptor, HER2, HER3, and HER4 are tyrosine kinase receptors and members of the ERBB family. These proteins act as homo- or heterodimers and contribute to cancer proliferation and progression.<sup>1</sup> Both *EGFR* and *HER2* act as oncogenic drivers in several tumor types.

The incidence of *EGFR*-activating mutations of exon 19 deletions or L858R point mutation is the most frequent (80%) of all *EGFR* mutations in NSCLC.<sup>2,3</sup> Such tumors are sensitive to *EGFR*-TKIs.<sup>4–10</sup> *Human epidermal growth factor receptor type 2* aberrations, such as amplification, mutations, or overexpression, are found in various cancers, among which *HER2* amplification in breast and gastric cancers have been well investigated. Several anti-*HER2* agents are used in both *HER2*-positive breast and gastric cancers.<sup>11</sup>

Approximately 2%–4% of patients with NSCLC harbor *HER2* exon 20 insertions.<sup>12</sup> However, a limited efficacy is seen in these patients using approved *HER2*-TKIs.<sup>13</sup> Additionally, *EGFR* exon 20 insertions, accounting for approximately 0.3%–3.7% of all NSCLC cases,<sup>12</sup> show poor response to *EGFR*-TKI monotherapies.<sup>13–17</sup> Recently, several *EGFR* targeting drugs, such as poziotinib, mobocertinib/TAK-788, and amivantamab/JNJ-61186372 (anti-*EGFR*-MET bispecific Ab), have shown promising results against NSCLC with *EGFR* exon 20 insertions.<sup>13,18–20</sup> In NSCLC patients with *HER2* mutations, [fam-] trastuzumab deruxtecan/DS-8201a also showed promising results.<sup>21</sup>

Approximately 25%–40% of NSCLC and 15%–30% of breast cancer patients develop brain metastases.<sup>22,23</sup> Although several promising drugs for these cancers exist, no blood–brain barrier-penetrable TKIs or Ab–drug conjugates have been approved for NSCLC with *HER2/EGFR* exon 20 insertions.<sup>12</sup> *Epidermal growth factor receptor* amplification and mutations, including *EGFR* vIII mutations with WT kinase domain, have also been observed in glioblastomas.<sup>24</sup> Hence, a dire need for a brain-penetrable pan-ERBB inhibitor active against *HER2/EGFR*, including exon 20 insertion mutations and *EGFR* vIII mutation, prevails.

Here, we evaluated the effects and benefits of TAS2940 against cancer cells harboring *HER2/EGFR* aberrations, using in vivo xenograft mouse models.

## 2 | MATERIALS AND METHODS

### 2.1 | Compounds

TAS2940 fumarate, hereafter referred to as TAS2940, was used for all our experiments. The doses are presented as free base equivalents. TAS2940 was synthesized at Taiho Pharmaceutical Co., Ltd., as per the procedure described in (Figure S1). The structure was confirmed using electrospray ionization–mass spectrometry and nuclear magnetic resonance spectroscopy, and its purity was determined to be greater than 99% by HPLC. Lapatinib, afatinib, neratinib, and osimertinib were purchased from LC Laboratories, Selleck Chemicals,

Hangzhou APIChem Technology Co., Ltd, and ChemScene LLC, respectively; tucatinib and poziotinib were obtained from Haoyuan ChemExpress Co., Ltd. Each compound was dissolved in DMSO for in vitro assays. For in vivo experiments, TAS2940 was suspended in 0.5% HPMC, while poziotinib and afatinib were suspended in a vehicle solution as described earlier.<sup>13,25</sup>

### 2.2 | Enzyme assay

The kinase assays using the ERBB inhibitors were outsourced to SignalChem Lifesciences Corporation for *HER2* mutations or Carna Biosciences, Inc. for *HER2/EGFR* WT and *EGFR* mutations; the phosphorylation of each peptide using the ADP-Glo assay or Off-chip Mobility Shift Assay was evaluated. The  $IC_{50}$  value of each compound against each enzyme was calculated from three independent experiments. The ATP concentration in the assay was set around  $K_m$  value of each kinase for ATP. The enzymatic inhibitory effect of poziotinib against *EGFR* was provided from Carna Biosciences Inc. (unpublished data). The kinase selectivity of TAS2940 and poziotinib was assessed against a panel of 257 kinases (Carna Biosciences Inc.); phosphorylation of each peptide was quantified using the mobility shift or the IMAP assays. Inhibition rates (% inhibition) of TAS2940 and poziotinib against 254 kinases were determined at 100× the concentration of each  $IC_{50}$  value against WT *HER2*, and the  $IC_{50}$  values against off-target enzymes were calculated using singlet assay in duplicate mode.

### 2.3 | Mass spectrometry analysis

For intact MS analysis, recombinant human *HER2* protein and TAS2940 were incubated, followed by LC-MS analysis using the Xevo G2-S QToF system (Waters Corporation). For peptide mapping analysis, recombinant human *HER2* protein and TAS2940 were incubated. After protein digestion, the peptide–compound complex was evaluated as described in Appendix S1.

### 2.4 | Cell lines and growth inhibition assay

MCF10A cell lines stably expressing WT or mutated *HER2/EGFR* genes were established by Dr. Motoki Takagi of Fukushima Medical University as described previously.<sup>26</sup> NCI-H1975 *EGFR* D770\_N771insSVD\_Luc cells were established as reported previously.<sup>27</sup> PDX35 fragments, patient-derived glioblastoma xenograft with *EGFR* vIII mutations, were provided by the Central Institute for Experimental Animals. The information of other cell lines is provided in Appendix S1.

All cell lines were authenticated using short tandem repeat profiling before or after use. The genetically engineered cells were confirmed to match with each parent cell line.

For growth inhibition assay, cell lines were incubated with test compounds for 3 days, and cellular viability was measured as demonstrated in Table S1 and Appendix S1.

## 2.5 | Western blot analysis

Cell lysates prepared from in vitro cultured cells or in vivo xenograft tumor cells were separated using SDS-PAGE and transferred to PVDF membranes. After treatment with primary and secondary Abs, chemiluminescence images were captured by a charge-coupled device imager as shown in Appendix S1.

## 2.6 | In-Cell Western assay

MCF10A cell lines were plated into 96-well plates at a density of  $1.0 \times 10^4$  cells/well. After 4 h of exposure to the compounds, In-Cell Western (Cell Signaling Technology) assay was carried out as previously described.<sup>28</sup>

## 2.7 | Pharmacokinetics

The plasma concentration of TAS2940 was detected in male BALB/cAJcl-nu/nu mice following a single or multiple oral treatments for 7 days at 6.3, 12.5, and 25.0 mg/kg in 0.5 w/v% HPMC solution. Blood samples were collected in tubes containing heparin solution at 0.25, 0.5, 1, 2, 4, 6, and 24 h postdose on day 1 and at pre- and postdose at 0.25, 0.5, 1, 2, 4, 6, and 24 h on day 7. The plasma samples obtained by centrifuging blood samples (18,600g, 3 min, 4°C) were deproteinized using ethanol containing an internal standard and filtered using centrifugation (890g, 5 min, 5°C). The filtrate was mixed with 50% acetonitrile solution, and the mixture was used for LC-MS/MS.

## 2.8 | Brain penetrability

The following compounds were given to male BALB/cAJcl-nu/nu mice: a single oral dose of lapatinib 50.0 mg/kg in 0.1 vol% Tween-80+0.5 w/v% HPMC solution, neratinib 40.0 mg/kg in 0.4 vol% Tween-80+0.5 w/v% methyl cellulose 400 solution, tucatinib 75.0 mg/kg in 0.1 N HCl+0.5 w/v% HPMC solution, poziotinib 1.0 mg/kg in 3 vol% Tween-80+20 vol% PEG400 solution, TAS2940 25.0 and 50.0 mg/kg in 0.5 w/v% HPMC solution, and osimertinib 25.0 mg/kg in 0.1 N HCl+0.5 w/v% HPMC solution. At an appropriate  $T_{\max}$  (1 h, lapatinib; 2 h, neratinib; 1 h, tucatinib; 0.25 h, poziotinib; 0.5 h, TAS2940; and 2 h, osimertinib), blood and brain tissues were collected. Plasma samples were obtained through blood centrifugation. The brain tissue samples were homogenized in 3× purified water. The plasma and brain homogenates were processed using the same method described above and subjected to LC-MS/MS analysis.

Unbound fractions of each compound in mouse plasma and brain homogenate samples were determined using the equilibrium

dialysis method. Brain tissue was homogenized in 3× PBS. TAS2940 was spiked at final concentrations of 0.2–20 μmol/L in plasma and 0.05–5 μmol/L in brain homogenates. Similarly, other compounds were spiked into mouse blank plasma and brain homogenates at final concentrations of 10 μmol/L. Spiked plasma and brain homogenates were dialyzed for 6 h at 37°C under 10% CO<sub>2</sub>. After incubation, the samples were processed as described earlier and injected into an LC-MS/MS system.

Brain penetrability of each compound was compared based on the unbound brain to unbound plasma concentration ratio ( $K_{p,uu,brain}$ ).

## 2.9 | In vivo efficacy studies

NCI-N87, MCF10A\_HER2/insYVMA\_v, NCI-H1975 EGFR D770\_N771insSVD ( $8 \times 10^6$  cells/mouse) cells, or PDX35 (approximately 8 mm<sup>3</sup> fragment/mouse) were subcutaneously implanted into 6-week-old male BALB/cAJcl-nu/nu mice (CLEA Japan Inc.). Cell suspensions were prepared with PBS for NCI-N87 and NCI-H1975 EGFR D770\_N771insSVD, or with 50% PBS and 50% Matrigel (BD Biosciences) for MCF10A\_HER2/insYVMA\_v. After reaching approximately 100–300 mm<sup>3</sup>, mice were randomly assigned to each group and TAS2940, poziotinib, or vehicle (0.5 w/v% HPMC) was given orally once daily for 14 days in each group ( $n = 6$ ), except to the PDX35 model, to which TAS2940, osimertinib, afatinib, or vehicle was given for 11 days in each group ( $n = 5$ ). The TV was calculated using the following formula:

$$TV(\text{mm}^3) = (\text{major axis}[\text{mm}]) \times (\text{minor axis}[\text{mm}])^2 / 2.$$

Bodyweight change in each mouse was monitored (Figure S2). In intracranial tumor xenograft models, NCI-N87-luc or NCI-H1975 EGFR D770\_N771insSVD\_Luc cells were intracranially transplanted into BALB/cAJcl-nu/nu mice ( $2.5 \times 10^5$  cells/mouse). After 3–4 weeks of implantation, luciferin was given intraperitoneally or intravenously. Total flux (radiance < photons/s [p/s] > in each pixel summed over each target area) values were measured using the IVIS Lumina II Imaging System (Perkin Elmer Inc.) to confirm tumor cell engraftment in the mouse brain. After grouping based on the total flux values, TAS2940, poziotinib, or vehicle was given once daily to mice in each group ( $n = 8–10$ ).

The MST in each group was calculated, and the log-rank test was used to compare survival experiences between groups. The statistical analysis was undertaken using Windows SAS system release 9.2 or 9.4 (SAS Institute Inc.) in an EXSUS (version 8 or 10; CAC Croit Corporation) environment.  $p < 0.05$  was considered statistically significant.

## 2.10 | Immunohistochemistry analysis

Brain samples intracranially transplanted with NCI-N87-luc cells were collected at 4 h after multiple dosing (3 days) of 25.0 mg/kg TAS2940 and stained as shown Appendix S1.

### 3 | RESULTS

#### 3.1 | TAS2940 is a highly potent selective inhibitor of ERBB

TAS2940 was discovered through compound-library screening and structure-based designing (Figure 1A). The mass of the HER2 cytoplasmic domain in the presence of TAS2940 was  $482.4 \pm 1.0$  Da, higher than that in its absence (Figure 1B), where the mass difference nearly corresponded to the molecular weight of TAS2940 (482.58 Da). Peptide mapping analysis indicated that TAS2940 was covalently bonded to the cysteine residue (Cys 805) of the recombinant human HER2 protein (Figure 1C).

The  $IC_{50}$  values of TAS2940 against WT HER2, HER2 V777L, and A775\_G776insYVMA were 5.6, 2.1, and 1.0 nmol/L, respectively (Figure 1D). TAS2940 inhibited both WT and mutant EGFRs (Figure 1E), as with poziotinib (Figure S3). By contrast, lapatinib inhibited WT HER2 more potently than HER2 mutant types (Figure 1D). We further evaluated the selectivity of TAS2940. Poziotinib inhibited 41 kinases at >50% of enzymatic activity at drug concentrations 100-fold that of the  $IC_{50}$  value of WT HER2 (Figure 1F, right panel and Table S2), whereas TAS2940 inhibited 10 kinases (Figure 1F, left panel and Table S2), indicating that TAS2940 is more selective than

poziotinib, as the former shows features of an irreversible pan-ERBB inhibitor.

#### 3.2 | TAS2940 broadly inhibits the phosphorylation of HER2/EGFR mutant cells and HER2/HER3 signaling continuously in HER2-positive cancer cells

TAS2940 considerably decreased WT and mutant phosphorylated HER2/EGFR in a dose-dependent manner after 4 h of drug treatment (Figure 2A, left panel). Phosphorylation of YVMA exon 20 insertions was strongly inhibited by TAS2940, which has a similar target engagement pattern to that of poziotinib (Figure 2A, right panel and Table 1). TAS2940 also potently inhibited phosphorylation of EGFR in HEK293 cells transiently expressing various EGFR exon 20 insertions after 6 h of treatment (Figure S4). TAS2940 treatment inhibited the phosphorylation of HER2, HER3, AKT, and ERK at concentrations of 10–30 nmol/L for 48 h (Figure 2B). The protein levels of B-cell lymphoma 2 interacting mediator of cell death (BIM) and cleaved PARP were markedly increased after treatment of SK-BR-3 cells with 10–100 nmol/L TAS2940 for 48 h, similar to the effect by poziotinib. Treatment with lapatinib and tucatinib at 30–300 nmol/L

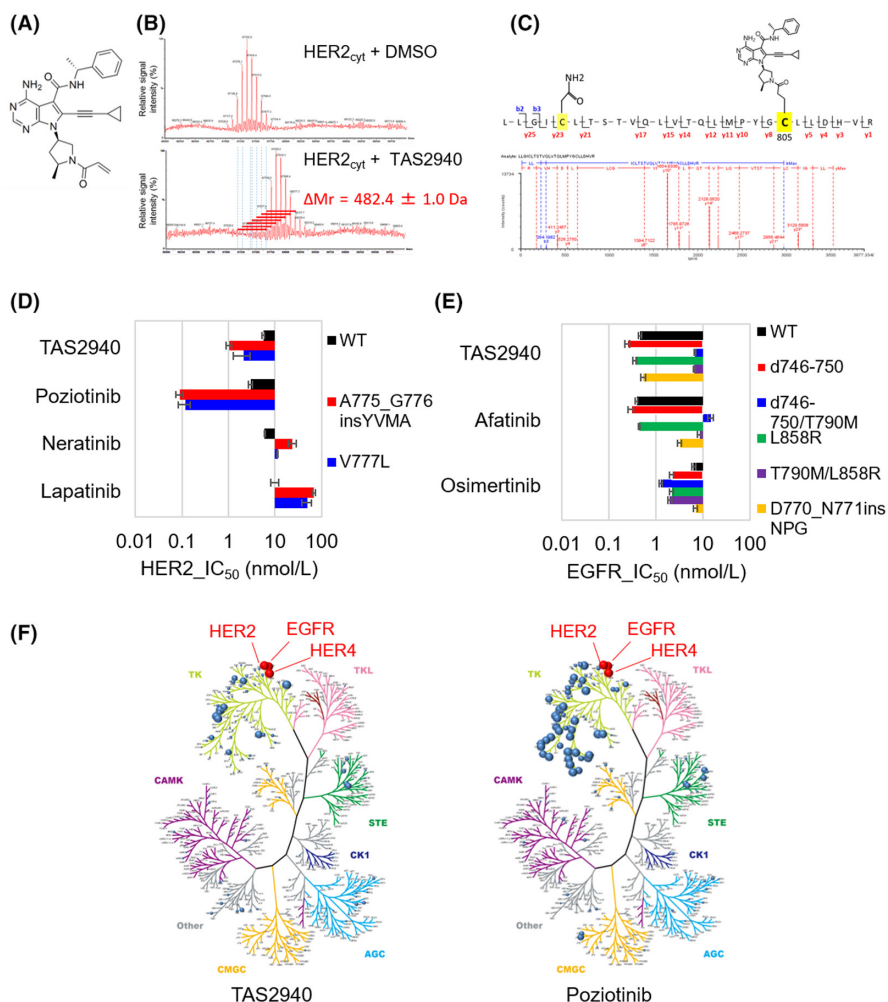


**FIGURE 1** TAS2940 is a covalent human epidermal growth factor receptor type 2 (HER2)/epidermal growth factor receptor (EGFR) inhibitor containing HER2/EGFR exon 20 insertions. (A) Chemical structure of TAS2940. (B) Liquid chromatography-mass spectrometry analysis of the recombinant human HER2 cytoplasmic domain (HER2<sub>cyt</sub>). (C) MS<sup>E</sup> spectrum confirmation for protease-digested recombinant human HER2 peptide (LLGICLTSTVQLVTQLMPYGCLLDHVR) with TAS2940. (D) Kinase inhibitory activity of TAS2940 and approved or investigational HER2/EGFR inhibitors on HER2. (E) Kinase inhibitory activity of TAS2940 and approved or investigational HER2/EGFR inhibitors on EGFR. The mean  $\pm$  SD of the  $IC_{50}$  value of each compound was calculated from three independent experiments. (F) Kinome inhibition plot of TAS2940 (left) and poziotinib (right).

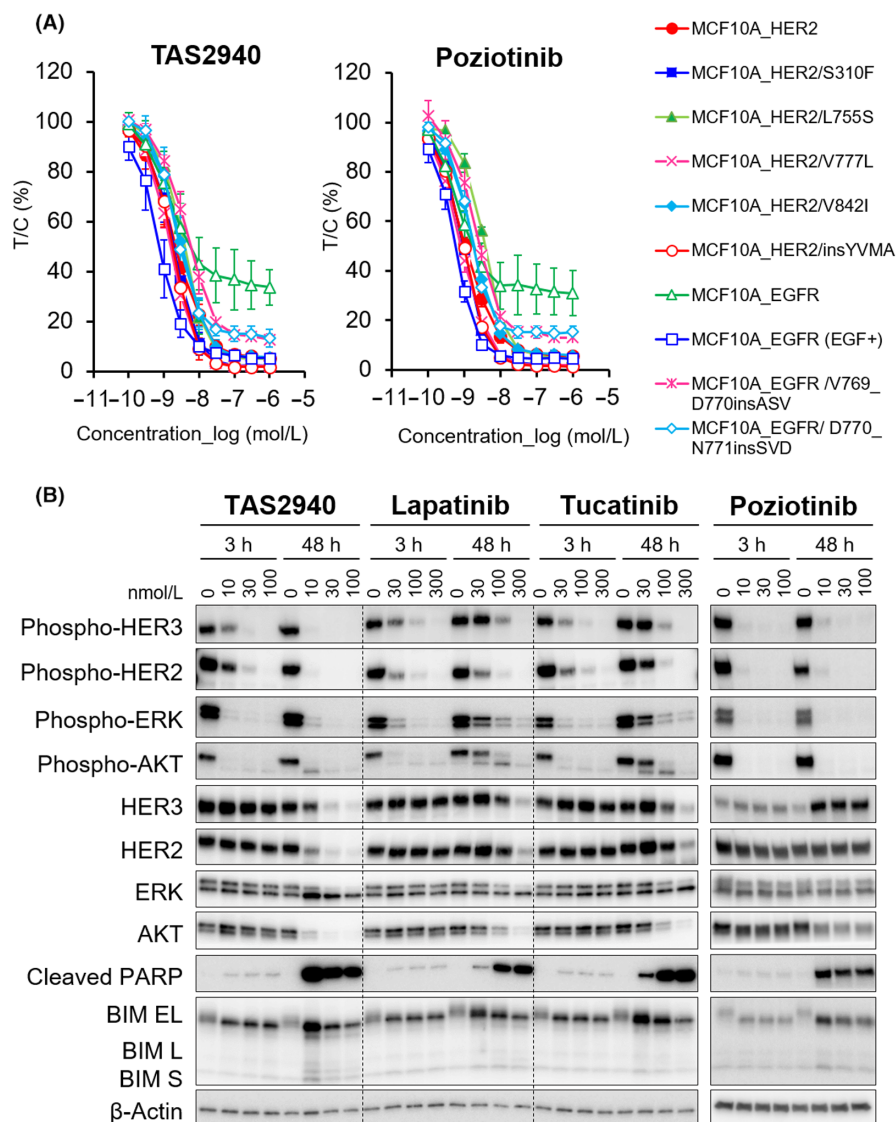


**FIGURE 2** TAS2940 shows higher selectivity for human epidermal growth factor receptor type 2 (HER2) and epidermal growth factor receptor (EGFR) aberrations. (A) The inhibitory effect of TAS2940 on the phosphorylation of HER2/EGFR in MCF10A cells stably expressing WT or mutant HER2/EGFR. The cells were cultured with TAS2940 or poziotinib and harvested for 4 h following treatment. Phosphorylation of HER2-Tyr1196 and EGFR-Tyr1068 was determined by the In-Cell Western assay. (B) Inhibition of the HER2 signaling pathway and effect of TAS2940, lapatinib, tucatinib, or poziotinib in the SK-BR-3 cell line. The cell line was treated by each compound for 3 or 48 h. Phosphorylated HER2, HER3, their downstream signaling factors, or apoptosis markers were detected by western blot analysis. BIM, B-cell lymphoma 2 interacting mediator of cell death; PARP, poly (ADP-ribose) polymerase.

also inhibited the phosphorylation of HER2, HER3, and their downstream proteins. However, at 48 h, the phosphorylation of HER3 and its downstream targets, AKT and ERK, was increased for the both HER2 inhibitors (Figure 2B).

### 3.3 | Effects of TAS2940 on cell proliferation with diverse EGFR and HER2 genetic alterations

As a control, lapatinib showed strong growth inhibitory effects on BT-474 and NCI-N87 cells harboring *HER2* amplification (Table 2). However, moderate or weak effects were observed in cells with *HER2* mutations and *EGFR* amplification and mutations. Neratinib and tucatinib inhibited the growth of *HER2* amplified cells. TAS2940 showed potent growth inhibition in all the cells harboring *EGFR/HER2* genetic aberrations, whereas almost no effect in NCI-H460 cells with *KRAS* mutation without *ERBB* genetic alteration was observed when examined at the maximal concentration of 1000 nmol/L. Consistent with enzymatic assay and PD analysis,

poziotinib showed similar growth inhibitory effects as TAS2940 in vitro.

### 3.4 | Pharmacokinetics and PD of TAS2940 in vivo

The plasma concentration–time profiles and pharmacokinetic parameters of TAS2940 at 6.3, 12.5, and 25.0 mg/kg were evaluated in male BALB/cAJcl-nu/nu mice after a single oral dose (Figure 3A, left) or multiple oral doses for 7 days (Figure 3A, right). The  $C_{max}$  and  $AUC_{last}$  values increased in a dose-dependent manner (Table S3). Apparent half-life values and  $C_{max}$  were 0.69–2.20 h and 601–3710 ng/ml, respectively (Table S3). We also measured phospho-HER2/3, phospho-AKT, and phospho-ERK levels in tumors as downstream key signaling PD markers after 1 h of TAS2940 treatment in NCI-N87-bearing nude mice xenograft models. As indicated in Figure 3B,C, dose-dependent inhibition of the PD markers was observed, and approximately 90% of inhibition was achieved when the xenograft tumor model was dosed at 25.0 mg/kg (Figure 3B).

**TABLE 1** Inhibitory concentration 50% (IC<sub>50</sub>) values of compounds for phosphorylation of WT or mutated human epidermal growth factor receptor type 2 (HER2)/epidermal growth factor receptor (EGFR).

Cell lines	IC <sub>50</sub> (nmol/L), mean ± SD	
	TAS2940	Poziotinib
MCF10A_HER2	2.27 ± 0.90	1.06 ± 0.13
MCF10A_HER2/S310F	1.98 ± 0.74	0.932 ± 0.038
MCF10A_HER2/L755S	3.74 ± 1.20	3.52 ± 0.18
MCF10A_HER2/V777L	1.54 ± 0.35	0.819 ± 0.121
MCF10A_HER2/V842I	3.28 ± 1.03	1.84 ± 0.24
MCF10A_HER2/ insYVMA	1.91 ± 0.84	0.956 ± 0.132
MCF10A_EGFR	9.38 ± 10.30	1.92 ± 0.99
MCF10A_EGFR (EGF+)	0.804 ± 0.311	0.576 ± 0.089
MCF10A_EGFR/ V769_D770insASV	5.64 ± 1.76	2.54 ± 0.35
MCF10A_EGFR/ D770_N771insSVD	2.98 ± 1.55	1.71 ± 0.25

Note: Inhibition of phospho-HER2 or phospho-EGFR was evaluated by 4 h of treatment of compounds with cells expressing WT and mutated HER2/EGFR, and then the IC<sub>50</sub> value was determined. Mean IC<sub>50</sub> values from three independent experiments are displayed with three significant digits, while the corresponding SD was rounded to the same number of decimal places as the mean.

Next, we evaluated PD markers to examine the dose-dependent change in target engagement by western blotting. Sustained inhibitions of phospho-HER2, phospho-HER3, and phospho-AKT were observed after 1–6 h of 25.0 mg/kg TAS2940 treatment. With respect to phospho-ERK, moderate inhibition was observed by the TAS2940 dosing. In parallel with the decrease in phospho-HER2/3 and phospho-AKT, cleaved PARP, as an indicator of apoptosis, increased in a time-dependent manner (Figure 3D).

### 3.5 | Antitumor efficacy of TAS2940 in a mouse subcutaneous model implanted with cancer cells with HER2/EGFR aberrations

Although NCI-N87 is a gastric cancer cell line, several in vivo xenograft models generated using NCI-N87 cells have been used to test the efficacies of HER2-targeting drugs approved for HER2 amplified breast cancer.<sup>29,30</sup> Therefore, we used the NCI-N87 xenograft subcutaneous tumor mouse model to initially assess the efficacy of TAS2940 against HER2 amplified cancer. Measurement of tumor volumes revealed dose-dependent antitumor effects in mice treated with either TAS2940 or poziotinib (Figure 4A). We found significant tumor regression at a dose of 12.5 mg/kg TAS2940. The maximal efficacy of TAS2940 was almost equivalent to that of poziotinib. We also confirmed the antitumor effects of TAS2940 and poziotinib in other xenograft subcutaneous tumor models: MCF10A\_HER2 ex20ins YVMA (Figure 4B), NSCLC H1975\_EGFR\_ex20ins SVD

**TABLE 2** Fifty percent growth inhibitory concentration (GI<sub>50</sub>) values of TAS2940 and other human epidermal growth factor receptor type 2 (HER2)/epidermal growth factor receptor (EGFR) inhibitors for a panel of human cell lines with ERBB1/2 amplification or mutations.

Cell line	Genetic alteration	GI <sub>50</sub> (nmol/L), mean ± SD							
		TAS2940	Lapatinib	Neratinib	Poziotinib	Tucatinib	Afatinib	Osimertinib	
BT-474	HER2 amplification	2.05 ± 0.48	12.1 ± 7.3	1.03 ± 0.69	0.508 ± 0.267	8.88 ± 8.19	2.42 ± 2.34	15.4 ± 12.0	
NCI-N87	HER2 amplification	0.891 ± 0.312	16.7 ± 10.0	0.946 ± 0.771	0.345 ± 0.159	12.2 ± 8.6	1.47 ± 0.81	13.5 ± 8.3	
MCF10A_HER2 / insYVMA	HER2 mutation (A775_G776 insYVMA)	23.3 ± 1.4	>1000	84.3 ± 9.0	8.27 ± 0.93	>1000	102 ± 17	>1000	
NCI-H1781	HER2 mutation (G776delinsVC)	5.85 ± 2.83	576 ± 282	15.4 ± 5.9	2.47 ± 1.35	229 ± 149	13.8 ± 8.7	82.0 ± 10.0	
A-431	EGFR amplification	8.64 ± 1.07	424 ± 29	35.8 ± 9.7	0.695 ± 0.174	>1000	9.33 ± 0.72	151 ± 30	
HCC827	EGFR mutation (delE746_A750)	2.13 ± 0.61	679 ± 211	292 ± 187	2.17 ± 0.75	>1000	2.25 ± 0.38	13.6 ± 10.0	
NCI-H1975	EGFR mutation (L858R and T790M)	37.50 ± 20.40	>1000	236 ± 147	14.2 ± 7.5	>1000	108 ± 40	13.8 ± 9.6	
NCI-H1975 EGFR D770_N771insSVD	EGFR mutation (EGFR D770_N771 insSVD)	8.71 ± 4.56	>1000	130 ± 60	3.87 ± 2.04	>1000	188 ± 53	154 ± 55	
NIH/3T3_EGFR vIII	EGFR vIII mutation	26.4 ± 2.3	>1000	114 ± 72	12.7 ± 15.1	>1000	184 ± 142	253 ± 56	
NCI-H460	KRAS mutation (Q61H)	>1000	>1000	860 ± 67	>1000	>1000	>1000	>1000	

Note: GI<sub>50</sub> values were determined in 3 days after the treatment with test compounds. Mean GI<sub>50</sub> values from three independent experiments are presented with the three significant digits.

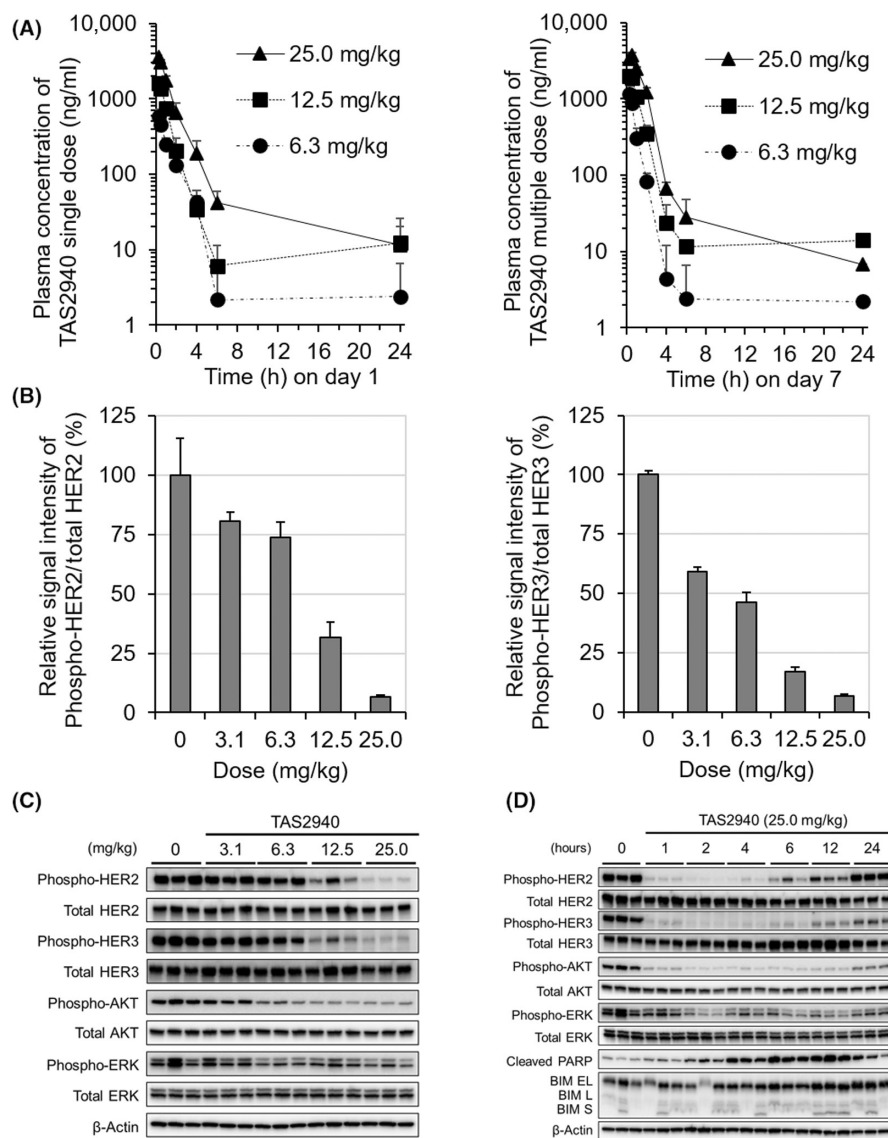


**FIGURE 3** Pharmacokinetics and pharmacodynamics of TAS2940 in NCI-N87 mouse xenograft model. (A) Plasma concentration profiles of TAS2940 after a single oral treatment (left panel) or multiple oral treatments for 7 days (right panel) in male BALB/cA/Jcl-nu/nu mice. Data are shown as the mean  $\pm$  SD ( $n = 3$ ). (B–D) Inhibition of phospho-human epidermal growth factor receptor type 2 (HER2), HER3, and their downstream molecules by TAS2940 was evaluated in NCI-N87 nude mouse xenograft model by western blot analysis. Using the samples collected at 1 h following treatment with TAS2940 at various concentrations, the chemiluminescence signal bands for phospho-HER2, HER2 protein, phospho-HER3, HER3 protein, and  $\beta$ -actin in (C) were subjected to semiquantitative analysis, and the phospho-HER2/HER2 and phospho-HER3/HER3 signal ratios were calculated (B). Duration of inhibitory activity against HER2 signaling was confirmed after treatment with TAS2940 at 25.0 mg/kg (D).

(Figure 4C), and glioblastoma PDX35 harboring *EGFR* vIII (Figure 4D). In H1975 *EGFR* ex20ins SVD, tumor growth retardation was observed, whereas growth suppression or tumor regression was seen in the other two models.

### 3.6 | Brain penetration and antitumor activity of TAS2940 in intracranial xenograft tumor models using HER2 amplification and *EGFR* exon 20 insertion cells

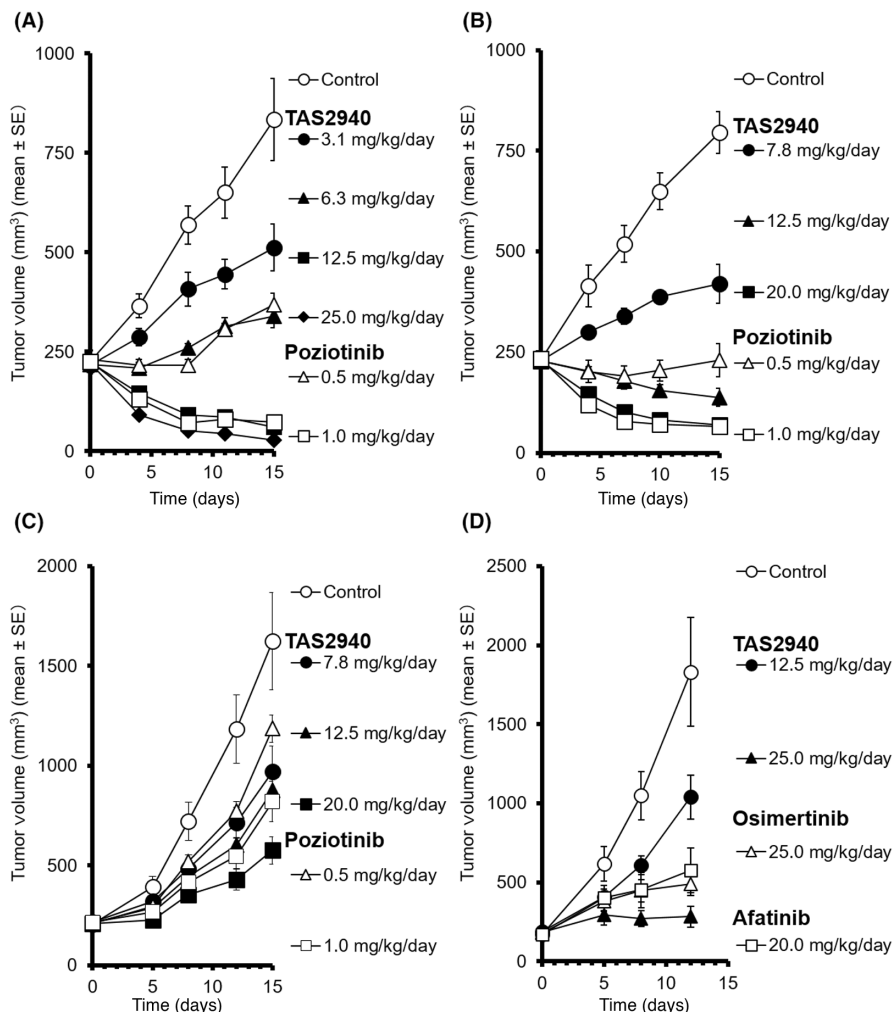
As TAS2940 was designed to penetrate the brain, we assessed the  $K_{p,uu,brain}$  of TAS2940 using male BALB/cA/Jcl-nu/nu mice. Brain penetrability of several HER inhibitors, other than TAS2940, was also evaluated. As shown in Figure 5A, average  $K_{p,uu,brain}$  values of lapatinib, neratinib, tucatinib, and poziotinib were comparable. However, these values were much lower than that of osimertinib (0.4), which is known to be brain-penetrable and effective in brain metastasis in clinical settings. The average  $K_{p,uu,brain}$  value of TAS2940 at 25.0 mg/kg was higher than that of other HER inhibitors, except osimertinib.

The maximum  $K_{p,uu,brain}$  value of TAS2940 reached approximately 0.3, indicating that TAS2940 has optimal brain penetrability.

We then evaluated the efficacy of TAS2940 in an intracranial NCI-N87 xenograft model. As shown in Figure 5B,C, notable tumor regression was shown after treatment with 20.0 or 25.0 mg/kg/day of TAS2940 for 21 days. However, poziotinib, which showed tumor regression in the subcutaneous model, failed to show tumor regression in this model due to its limited brain penetrability. Moreover, we examined several dosing schedules of TAS2940 in this intracranial model. Continuous and alternate-day administration (quaque otra die, QOD) triggered tumor shrinkage, and 4 days-on/3 days-off administration induced tumor growth inhibition (Figure 5D). A reduction in the phosphorylated HER2 and Ki-67 signals was observed on day 3 of TAS2940 treatment (Figure 5E), indicating that the action of TAS2940 is mediated through phospho-HER2 inhibition.

We also investigated the efficacy of TAS2940 in an intracranial xenograft model generated using NCI-H1975\_EGFR\_exon20ins\_SVD cells harboring the luciferase gene, allowing the measurement of tumor volume using a bioluminescent assay. Mice were treated

**FIGURE 4** Antitumor activity of TAS2940 in multiple mouse xenograft models harboring several *human epidermal growth factor receptor type 2 (HER2)/epidermal growth factor receptor (EGFR)* aberrations. TAS2940, poziotinib, or vehicle was given orally once daily for 14 days in subcutaneous xenograft models bearing (A) NCI-N87, (B) MCF10A\_HER2/insYVMA\_v, or (C) NSCLC NCI-H1975 EGFR D770\_N771insSVD. (D) TAS2940, afatinib, osimertinib, or vehicle was given orally once daily for 11 days in subcutaneous xenograft models bearing glioblastoma PDX35. Data are shown as the mean  $\pm$  SE ( $n = 6$  in A–C;  $n = 5$  in D).



with TAS2940 for up to 39 days. On day 47, tumor volumes decreased, as observed with the NCI-N87 intracranial model. Survival studies also demonstrated the efficacy of 25.0 mg/kg TAS2940 (Figure 5F,  $p = 0.0059$ ; MST of TAS2940 group, 61 days; MST of control group, 47 days). These results illustrate the potential benefit of TAS2940 in patients with brain metastasis.

## 4 | DISCUSSION

Here, we showed that TAS2940 is a potent, selective, and orally bioavailable pan-ERBB inhibitor with antitumor efficacy against cancers with a variety of *HER2/EGFR* mutations and amplifications both in vitro and in vivo. Although a few pan-ERBB TKIs have shown similar inhibition spectra for the *EGFR* and *HER2* genes,<sup>13</sup> TAS2940 is unique as it possesses higher brain penetrability and shows the characteristic inhibition spectra for *EGFR* and *HER2* aberrations, as shown herein.

Small molecule compounds with high brain penetrability have shown to be effective against brain metastasis.<sup>31</sup> Additionally, a link between *EGFR* mutations and the likelihood of brain metastases exists; for instance, NSCLC with common *EGFR* mutations has a higher prevalence of brain metastasis compared with other tumor

types.<sup>32</sup> Osimertinib has shown similar clinical effects in both patients with and without brain metastasis<sup>31</sup> due to its good brain penetrability (approximately 0.21  $K_{p,uu,brain}$  in rodents).<sup>33</sup> Another example is the ALK inhibitor, lorlatinib, with a  $K_{p,uu,brain}$  value of 0.21 in rodents, showing an efficacy similar to that of osimertinib against brain metastasis. Lorlatinib has also shown efficacy in pre-clinical models and clinical settings.<sup>34–36</sup> Conversely, other *EGFR* TKIs with lower  $K_{p,uu,brain}$  values (afatinib, 0.0062; poziotinib, 0.06) in rodents showed highly limited efficacy in patients with brain metastasis. These data on other TKIs indicate that TAS2940, with a  $K_{p,uu,brain}$  value of approximately 0.3, could be brain penetrable in humans and might show efficacy against primary and metastatic brain tumors.

Although several pan-ERBB inhibitors have been developed, such as afatinib and dacomitinib for NSCLC with *EGFR* sensitizing mutations and neratinib for *HER2*-positive breast cancer,<sup>37</sup> most inhibitors are ineffective against *EGFR/HER2* exon 20 insertion. Afatinib, for instance, was evaluated for lung cancer with *EGFR* exon 20 insertion in clinical trials; however, the efficacy seen in the trials was limited.<sup>15</sup> Among the pan-ERBB inhibitors examined in clinical trials to date, poziotinib has shown relatively good clinical benefits in NSCLC with *EGFR/HER2* exon 20 insertions.<sup>13,18,38</sup> Poziotinib has shown greater activity against *EGFR/HER2* exon 20 insertions than



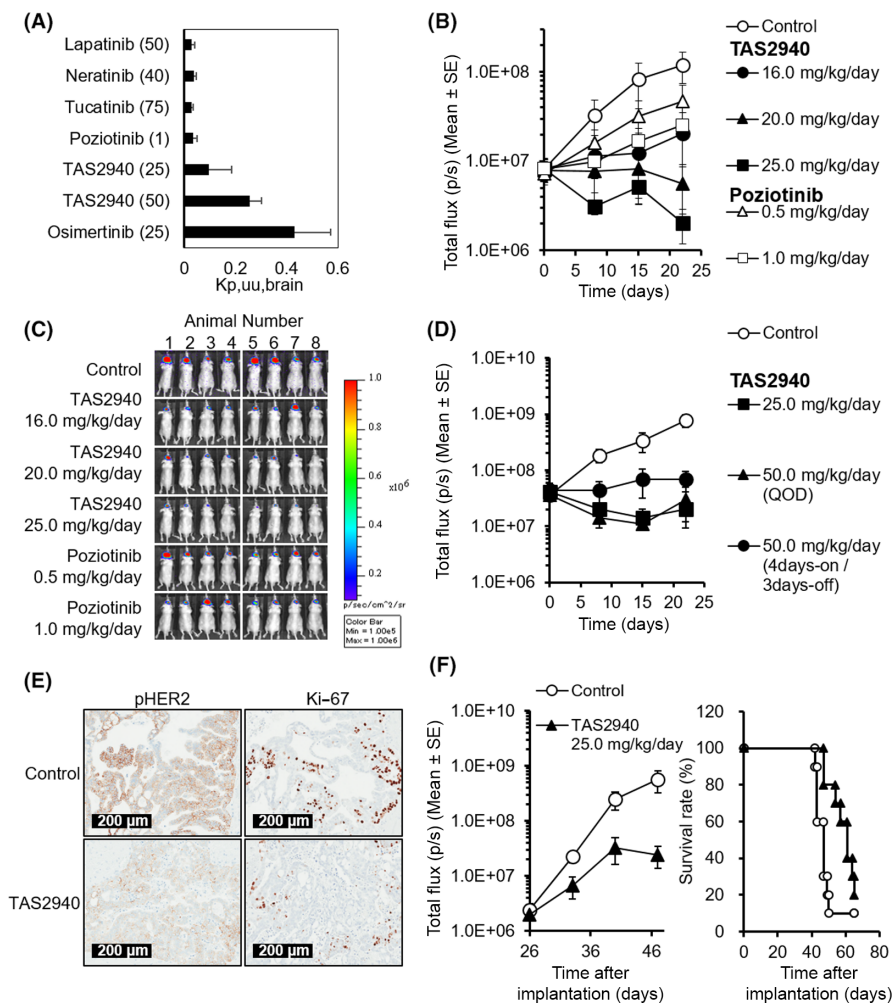


**FIGURE 5** Brain penetrability and antitumor activity of TAS2940 in NCI-N87-luc (*human epidermal growth factor receptor type 2 [HER2] amp*) and NCI-H1975\_EGFR ex20insSVD-luc intracranial brain metastasis models. (A) The unbound concentration in the brain to the unbound concentration in plasma ratio ( $K_{p,uu,brain}$ ) values of lapatinib, neratinib, tucatinib, pozotinib, TAS2940, and osimertinib ( $n = 3$ ). (B) Total flux (p/s) values in the NCI-N87-luc intracranial model. (C) Bioluminescence images obtained on day 22. (D) Total flux (p/s) values in the NCI-N87-luc intracranial model with different dosing schedules of TAS2940. (E) Target inhibition of TAS2940 assessed by phospho-HER2 and growth fraction assessed by Ki-67 in the NCI-N87-luc model. (F) Antitumor activity and survival benefit of TAS2940 in the NCI-H1975\_EGFR ex20ins SVD-luc intracranial nude mouse model. Data are presented as the mean  $\pm$  SE ( $n = 8$  in B,C;  $n = 6$  in D). EGFR, human epidermal growth factor receptor.

the approved EGFR TKIs as it tightly binds to the sterically hindered drug-binding pocket of such mutated proteins.<sup>13</sup> TAS2940 showed potent growth inhibition and target inhibition in cell lines with EGFR exon 20 insertions similar to that of pozotinib, suggesting similar structural characteristics.

Our kinase enzymatic assays showed that TAS2940 has a higher selectivity than pozotinib. As TAS2940 causes minimal inhibition of kinases other than those of the HER family, it will show reduced toxicity in clinical settings. Additionally, TAS2940 shows better brain penetration than pozotinib, possessing a higher potential against brain metastasis with a higher CNS response.

Tucatinib has shown clinical benefits against brain metastasis in HER2-positive breast cancer patients,<sup>39</sup> attributed to one of its metabolites being brain-penetrative. Compared with tucatinib, an ATP competitive-reversible inhibitor, TAS2940, a covalent inhibitor, shows more durable inhibition of the HER2/HER3 signaling axis and more potent antitumor effects. Another feature that differentiates TAS2940 from tucatinib is its HER2 mutation-specific inhibition pattern. This makes TAS2940 clinically relevant as the HER2 exon 20 insertion accounts for up to 70% of lung cancers with HER2 mutations, and treatment of these cancers is an unmet medical need. Our in vitro assay as well as in vivo efficacy data have shown that TAS2940, unlike tucatinib, is effective in cancer

models with HER2 exon 20 insertion and EGFR aberrations. These features of TAS2940 make it a unique therapeutic option for cancers with ERBB aberrations.

As lung and breast cancers with either EGFR or HER2 aberrations show a higher prevalence of brain metastasis,<sup>22,32</sup> brain penetrability is a key feature of candidate compounds that will determine efficacy. As glioblastoma with EGFR amplification or mutations as well as lung cancers having HER2 exon 20 insertion have no approved drugs to date, developing brain-penetrable EGFR/HER2 inhibitors is essential to fulfill such unmet medical needs. With a phase I trial ongoing (NCT04982926), our findings provide a strong rationale for evaluating TAS2940 in patients with HER2/EGFR aberrations, including those with brain metastases or brain tumors.

In conclusion, our results indicate that TAS2940 is a promising therapeutic option for breast and lung cancers with brain metastases harboring HER2/EGFR aberrations and for glioblastoma with EGFR aberrations.

#### AUTHOR CONTRIBUTIONS

Conception and design: K.O., S.S.K., and S.M. Development of methodology: K.O., H.A., S.T., A.M., S.T., and T.S. Acquisition of data: K.O., H.A., S.T., M.N., A.M., K.F., A.O., S.T., and T.S. Analysis and interpretation of data: K.O., H.A., S.T., and S.T. Writing, review, and/or

revision of the manuscript: K.O., S.S.K., and S.M. Administrative, technical, or material support: K.O. Study supervision: S.S.K. and S.M. Chemical design and synthesis: M.N.

## ACKNOWLEDGMENTS

The authors thank Drs. Teruhiro Utsugi, Kazuhiko Yonekura, Yoshikazu Iwasawa, Kazutaka Miyadera, Kenichi Matsuo, Shuichi Okubo, Naoki Matsumoto, and Kazuo Yamamoto for their insightful discussions. The authors also thank all the departments at the Discovery and Preclinical Research Division of Taiho Pharmaceutical Co., Ltd for the support they provided for this work.

## FUNDING INFORMATION

This study was funded by Taiho Pharmaceutical Co., Ltd., Japan.

## DISCLOSURE

S.S.K. reports research support from Boehringer Ingelheim, MiNA Therapeutics, Janssen, MiRXES, and Taiho Pharmaceutical Co., Ltd., as well as personal fees (honoraria) from Boehringer Ingelheim, Bristol Meyers Squibb, AstraZeneca, Chugai Pharmaceutical, and Takeda Pharmaceuticals, all outside of the submitted work. The other authors are employees of Taiho Pharmaceutical Co., Ltd.

## ETHICS STATEMENT

Approval of the research protocol by an institutional review board: N/A.

Informed consent: N/A.

Registry and the registration no. of the study/trial: [Clinicaltrials.gov](https://clinicaltrials.gov/ct2/show/study/NCT04982926) identifier: NCT04982926.

Animal studies: All animal experiments were performed under the regulations of the Institutional Animal Care and Use Committee of Taiho Pharmaceutical Co., Ltd.

## ORCID

Kei Oguchi  <https://orcid.org/0000-0003-3339-9583>

Susumu S. Kobayashi  <https://orcid.org/0000-0003-2262-4001>

## REFERENCES

- Artega CL, Sliwkowski MX, Osborne CK, Perez EA, Puglisi F, Gianni L. Treatment of HER2-positive breast cancer: current status and future perspectives. *Nat Rev Clin Oncol*. 2011;9(1):16-32.
- Shigematsu H, Lin L, Takahashi T, et al. Clinical and biological features associated with epidermal growth factor receptor gene mutations in lung cancers. *J Natl Cancer Inst*. 2005;97(5):339-346.
- Costa DB. Kinase inhibitor-responsive genotypes in EGFR mutated lung adenocarcinomas: moving past common point mutations or indels into uncommon kinase domain duplications and rearrangements. *Transl Lung Cancer Res*. 2016;5(3):331-337.
- Maemondo M, Inoue A, Kobayashi K, et al. Gefitinib or chemotherapy for non-small-cell lung cancer with mutated EGFR. *N Engl J Med*. 2010;362(25):2380-2388.
- Mitsudomi T, Morita S, Yatabe Y, et al. Gefitinib versus cisplatin plus docetaxel in patients with non-small-cell lung cancer harbouring mutations of the epidermal growth factor receptor (WJTOG3405): an open label, randomised phase 3 trial. *Lancet Oncol*. 2010;11(2):121-128.
- Zhou C, Wu YL, Chen G, et al. Erlotinib versus chemotherapy as first-line treatment for patients with advanced EGFR mutation-positive non-small-cell lung cancer (OPTIMAL, CTONG-0802): a multicentre, open-label, randomised, phase 3 study. *Lancet Oncol*. 2011;12(8):735-742.
- Rosell R, Carcereny E, Gervais R, et al. Erlotinib versus standard chemotherapy as first-line treatment for European patients with advanced EGFR mutation-positive non-small-cell lung cancer (EURTAC): a multicentre, open-label, randomised phase 3 trial. *Lancet Oncol*. 2012;13(3):239-246.
- Sequist LV, Yang JC, Yamamoto N, et al. Phase III study of afatinib or cisplatin plus pemetrexed in patients with metastatic lung adenocarcinoma with EGFR mutations. *J Clin Oncol*. 2013;31(27):3327-3334.
- Wu YL, Zhou C, Hu CP, et al. Afatinib versus cisplatin plus gemcitabine for first-line treatment of Asian patients with advanced non-small-cell lung cancer harbouring EGFR mutations (LUX-lung 6): an open-label, randomised phase 3 trial. *Lancet Oncol*. 2014;15(2):213-222.
- Yi L, Fan J, Qian R, Luo P, Zhang J. Efficacy and safety of osimertinib in treating EGFR-mutated advanced NSCLC: a meta-analysis. *Int J Cancer*. 2019;145(1):284-294.
- Yan M, Parker BA, Schwab R, Kurzrock R. HER2 aberrations in cancer: implications for therapy. *Cancer Treat Rev*. 2014;40(6):770-780.
- Baraibar I, Mezquita L, Gil-Bazo I, Planchard D. Novel drugs targeting EGFR and HER2 exon 20 mutations in metastatic NSCLC. *Crit Rev Oncol Hematol*. 2020;148:102906.
- Robichaux JP, Elamin YY, Tan Z, et al. Mechanisms and clinical activity of an EGFR and HER2 exon 20-selective kinase inhibitor in non-small cell lung cancer. *Nat Med*. 2018;24(5):638-646.
- Yasuda H, Park E, Yun CH, et al. Structural, biochemical, and clinical characterization of epidermal growth factor receptor (EGFR) exon 20 insertion mutations in lung cancer. *Sci Transl Med*. 2013;5(216):216ra177.
- Yang JCH, Sequist LV, Geater SL, et al. Clinical activity of afatinib in patients with advanced non-small-cell lung cancer harbouring uncommon EGFR mutations: a combined post-hoc analysis of LUX-lung 2, LUX-lung 3, and LUX-lung 6. *Lancet Oncol*. 2015;16(7):830-838.
- Wu JY, Wu SG, Yang CH, et al. Lung cancer with epidermal growth factor receptor exon 20 mutations is associated with poor gefitinib treatment response. *Clin Cancer Res*. 2008;14(15):4877-4882.
- Naidoo J, Sima CS, Rodriguez K, et al. Epidermal growth factor receptor exon 20 insertions in advanced lung adenocarcinomas: clinical outcomes and response to erlotinib. *Cancer*. 2015;121(18):3212-3220.
- Remon J, Hendriks LEL, Cardona AF, Besse B. EGFR exon 20 insertions in advanced non-small cell lung cancer: a new history begins. *Cancer Treat Rev*. 2020;90:102105.
- Riely GJ, Neal JW, Camidge DR, et al. Activity and safety of mobocertinib (TAK-788) in previously treated non-small cell lung cancer with EGFR exon 20 insertion mutations from a phase I/II trial. *Cancer Discov*. 2021;11(7):1688-1699.
- Yun J, Lee SH, Kim SY, et al. Antitumor activity of amivantamab (JNJ-61186372), an EGFR-MET bispecific antibody, in diverse models of EGFR exon 20 insertion-driven NSCLC. *Cancer Discov*. 2020;10(8):1194-1209.
- Li BT, Smit EF, Goto Y, et al. Trastuzumab deruxtecan in HER2-mutant non-small-cell lung cancer. *N Engl J Med*. 2022;386(3):241-251.
- Witzel I, Oliveira-Ferrer L, Pantel K, Müller V, Wikman H. Breast cancer brain metastases: biology and new clinical perspectives. *Breast Cancer Res*. 2016;18(1):8.
- Abdallah SM, Wong A. Brain metastases in non-small-cell lung cancer: are tyrosine kinase inhibitors and checkpoint inhibitors now viable options? *Curr Oncol*. 2018;25(Suppl 1):S103-S114.

24. An Z, Aksoy O, Zheng T, Fan QW, Weiss WA. Epidermal growth factor receptor and EGFRvIII in glioblastoma: signaling pathways and targeted therapies. *Oncogene*. 2018;37(12):1561-1575.
25. Li D, Ambrogio L, Shimamura T, et al. BIBW2992, an irreversible EGFR/HER2 inhibitor highly effective in preclinical lung cancer models. *Oncogene*. 2008;27(34):4702-4711.
26. Hoshi H, Hiyama G, Ishikawa K, et al. Construction of a novel cell-based assay for the evaluation of anti-EGFR drug efficacy against EGFR mutation. *Oncol Rep*. 2017;37(1):66-76.
27. Hasako S, Terasaka M, Abe N, et al. TAS6417, a novel EGFR inhibitor targeting exon 20 insertion mutations. *Mol Cancer Ther*. 2018;17(8):1648-1658.
28. Ito K, Nishio M, Kato M, et al. TAS-121, a selective mutant EGFR inhibitor, shows activity against tumors expressing various EGFR mutations including T790M and uncommon mutations G719X. *Mol Cancer Ther*. 2019;18(5):920-928.
29. Ogitani Y, Aida T, Hagihara K, et al. DS-8201a, a novel HER2-targeting ADC with a novel DNA topoisomerase I inhibitor, demonstrates a promising antitumor efficacy with differentiation from T-DM1. *Clin Cancer Res*. 2016;22(20):5097-5108.
30. Kulukian A, Lee P, Taylor J, et al. Preclinical activity of HER2-selective tyrosine kinase inhibitor tucatinib as a single agent or in combination with trastuzumab or docetaxel in solid tumor models. *Mol Cancer Ther*. 2020;19(4):976-987.
31. Soria JC, Ohe Y, Vansteenkiste J, et al. Osimertinib in untreated EGFR-mutated advanced non-small-cell lung cancer. *N Engl J Med*. 2018;378(2):113-125.
32. Offin M, Feldman D, Ni A, et al. Frequency and outcomes of brain metastases in patients with HER2-mutant lung cancers. *Cancer*. 2019;125(24):4380-4387.
33. Colclough N, Chen K, Johnström P, et al. Preclinical comparison of the blood-brain barrier permeability of osimertinib with other EGFR TKIs. *Clin Cancer Res*. 2021;27(1):189-201.
34. Johnson TW, Richardson PF, Bailey S, et al. Discovery of (10R)-7-amino-12-fluoro-2,10,16-trimethyl-15-oxo-10,15,16,17-tetrahydro-2H-8,4-(m etheno)pyrazolo[4,3-h][2,5,11]-benzoxa diazacyclotetradecine-3-carbonitrile (PF-06463922), a macrocyclic inhibitor of anaplastic lymphoma kinase (ALK) and c-ROS oncogene 1 (ROS1) with preclinical brain exposure and broad-spectrum potency against ALK-resistant mutations. *J Med Chem*. 2014;57(11):4720-4744.
35. Zou HY, Friboulet L, Kodack DP, et al. PF-06463922, an ALK/ROS1 inhibitor, overcomes resistance to first and second generation ALK inhibitors in preclinical models. *Cancer Cell*. 2015;28(1):70-81.
36. Shaw AT, Solomon BJ, Chiari R, et al. Lorlatinib in advanced ROS1-positive non-small-cell lung cancer: a multicentre, open-label, single-arm, phase 1-2 trial. *Lancet Oncol*. 2019;20(12):1691-1701.
37. Roskoski RJ. Orally effective FDA-approved protein kinase targeted covalent inhibitors (TCIs). *Pharmacol Res*. 2021;165:105422.
38. Le X, Cornelissen R, Garassino M, et al. Poziotinib in non-small-cell lung cancer harboring HER2 exon 20 insertion mutations after prior therapies: ZENITH20-2 trial. *J Clin Oncol*. 2022;40(7):710-718.
39. Lin NU, Borges V, Anders C, et al. Intracranial efficacy and survival with tucatinib plus trastuzumab and capecitabine for previously treated HER2-positive breast cancer with brain metastases in the HER2CLIMB trial. *J Clin Oncol*. 2020;38(23):2610-2619.

### SUPPORTING INFORMATION

Additional supporting information can be found online in the Supporting Information section at the end of this article.

**How to cite this article:** Oguchi K, Araki H, Tsuji S, et al. TAS2940, a novel brain-penetrable pan-ERBB inhibitor, for tumors with *HER2* and *EGFR* aberrations. *Cancer Sci*. 2023;114:654-664. doi: [10.1111/cas.15617](https://doi.org/10.1111/cas.15617)